



Poly(*o*-aminobenzyl alcohol) Films with and without Organic Compound on AISI 316 Surface; Synthesis and the Corrosion Performances

Ali Tuncay OZYILMAZ¹  , Begüm OZGEN¹,   Cumali CELIK²  

¹ Hatay Mustafa Kemal University, Faculty of Arts and Sciences, Department of Chemistry, Antakya / Hatay, Turkey

² University of Yalova, Yalova Vocational School, Property Protection and Security Department, Yalova, Turkey

Abstract: In this work, we obtained the anticorrosive properties of polymer films (SS/PABA and SS/PABA-ORG) synthesized on stainless steel surface by adding an organic substance to aniline derived *o*-aminobenzyl alcohol monomer synthesis medium. Firstly, we prepared the polymer coating bath by dissolving 0.15 M *o*-aminobenzyl alcohol monomer in the electrolyte solvent containing acetonitrile and 0.15 M LiClO₄. From this bath, poly (*o*-aminobenzyl alcohol) (PABA) film was synthesized in 30 segments by cyclic voltammetry (CV) technique at a scanning rate of 50 mV/s at a potential range of -0.20/1.80 V on the AISI 316 (SS) working electrode in contrast to the platinum electrode. For the synthesis of organic structure doped polymer film (PABA-ORG), we repeated the same synthesis process by dissolving C₂₁H₂₇NO_{2(k)} (ORG) at low concentration in the same bath. We investigated the corrosion performances of bare SS, SS/PABA, and SS/PABA-ORG substrates, using open circuit potential – time, anodic polarization, and AC impedance techniques in the solution of corrosion study. As a result, we observed that the organic additive added to the synthesis medium caused changes in the synthesis behavior of PABA. Corrosion performance tests showed that PABA and PABA-ORG films increased the corrosion protection performance of the SS electrode, and we observed a reduction of the corrosion rate of the SS electrode.

Keywords: corrosion; electropolymerization; *o*-aminobenzyl alcohol; AISI316.

Submitted: November 02, 2019. **Accepted:** March 24, 2020.

Cite this:

DOI: <https://doi.org/10.18596/jotcsa.641851>.

Corresponding author. E-mail: atuncay@mku.edu.tr.

INTRODUCTION

Corrosion is the physical and chemical erosion of metals and a momentous event that can cause serious harm to humanity despite today's developing technology. This phenomenon is because metals generally undergo electrochemical and chemical reactions within the atmosphere due to environmental factors. So the materials might receive severe damage. To prevent these damages and losses, researchers have been developing various methods and materials for years. Stainless steel, which is one of these materials, is resistant to many corrosive environments with its quality and

stable oxide layers formed by chromium and nickel metals in its compositions. However, it can corrode faster than expected in environments containing chloride and sulfate (1-3). AISI 316 series stainless sheets of steel, which are frequently preferred by the industry due to their cheapness, easy availability, and machinability, also have the disadvantage mentioned in such environments. Although there are many methods used to prevent this and increase the protective effect of stainless steel, conductive polymer coatings have received much attention in the literature recently (4-10). In particular, polyaniline and its derivatives are conductive polymers that are frequently studied and

give fruitful results. The main characteristics of conductive polymers are their high conductivity, corrosion-resistant, and non-corrosive enough to be brought to the metal level.

Furthermore, their electrochemical coating on technical metals results in meager costs, under constant potential, constant current, and cyclic voltammetry. Besides, one of the commonly applied techniques in recent years is cyclic voltammetry. In this technique, after the monomer oxidation, the polymer film is converted into induction and oxidation forms during synthesis. After the monomer oxidation, there is a conversion of the polymer film into induction and oxidation forms during synthesis. As known, once most inorganic inhibitors are harmful to the environment, organic inhibitors containing amine groups are useful to prevent corrosion. Amine-based inhibitors compose a thin adsorbed layer on the substrate, and this layer has a polymeric structure and is extremely protective against corrosion (11-13). The research made in the literature shows that the organic structure can add to the matrix of conductive polymer films (14). This study aim is to investigate the anti-corrosive properties of poly (o-aminobenzyl alcohol) synthesized from an aniline derived monomer o-aminobenzyl alcohol on AISI 316 stainless steel. Also, we synthesized the polymer coating (PABA-ORG) obtained in a mixture solution including o-aminobenzyl alcohol (ABA) and 2,6-di-*tert*-butyl-4- $\{(E)-[4-(4-hydroxyphenyl)imino]methyl\}$ phenol (M_w : 325.45) (ORG) compound having varying degree of hydrophobic chain length and the steric environment on AISI 316 stainless steel (SS) in $LiClO_4$ + acetonitrile medium. We explored the

corrosion performances of PABA coatings synthesized without and with 0.50 mM ORG compound in a 3.5 % NaCl solution. We evaluated the electrochemical measurement techniques of PABA polymer films with and without ORG compound obtained on SS (SS/PABA and SS/PABA-ORG) and bare SS.

MATERIALS AND METHODS

All electrochemical experiments were carried out with three-electrode in single-cell technique on CH Instruments electrochemical workstation. In the experiment cells, Ag/AgCl (3M KCl) and square platinum plate with a surface area of 0.25 cm² electrodes were reference and counter electrodes, respectively. AISI 316 electrode with a 0.50 cm² surface was the working electrode. Shortly before use, the SS electrode surface was carefully polished with 400 and 1200 grid abrasive paper, respectively, and washed with acetone+ethanol (1:1) mixture and bi-distilled water in this order. For the poly (o-aminobenzyl alcohol) (PABA) coating, we dissolved 0.15 M o-aminobenzyl alcohol monomer in acetonitrile (ACN) containing 0.15 M lithium perchlorate. Electropolymerization was carried out by cyclic voltammetry (CV) technique in 30 segments between -0.20 and 1.80 V at a scan rate of 50 mV s⁻¹. The fitting curves in the Nyquist and Bode diagrams in Figure 5c were analyzed using the ZView2 software. The structure of the organic compound named 0.50 mM 2,6-di-*tert*-butyl-4- $\{(E)-[4-(4-hydroxyphenyl)imino]methyl\}$ phenol (M_w : 325.45) joined to the PABA polymer film is given in Figure 1. The electropolymerization of PABA polymer film containing an organic compound (PABA-ORG) we applied the same process as that of PABA polymer film.

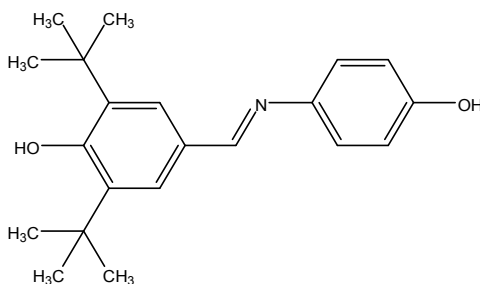


Figure 1: Chemical structure of the organic compound.

RESULTS AND DISCUSSION

Synthesis of the Polymeric Film

In this study, we synthesized PABA film in 0.15 M o-aminobenzyl alcohol (ABA) monomer dissolved in the solution of $LiClO_4$ in ACN by CV technique in one step. We coated Poly (o-aminobenzyl alcohol) (PABA) homopolymer films with and without organic compound (ORG) of 0.50 mM concentration on the

surface of the SS electrode using cyclic voltammetry at a scan rate of 50 mV/s. Figure 2 shows the film growth curves observed for SS in 0.15 M ABA (a) and 0.15 M ABA + 0.50 mM organic compound (ABA-ORG) (b) containing 0.15 M $LiClO_4$ + ACN solution. Film growth curves of electrodes obtained in both ORG compound-containing and ORG compound-free PABA medium, which are referred to here as SS/PABA-ORG and SS/PABA respectively,

showed in Figure 2. We obtained the works at a scan rate of $50 \text{ mV}\cdot\text{s}^{-1}$.

We carried out 30 segments for the synthesis of PABA or PABA-ORG coating on the SS electrode. Both coated electrodes exhibited entirely different electrochemical behavior in CV curves. The anodic current values increased after the potential value of 0.89 V during the first cycle in ABA monomer containing $\text{LiClO}_4 + \text{ACN}$ solution, while we observed them after the potential value of 0.88 V for $\text{LiClO}_4 + \text{ACN} + \text{ABA}$ monomer mixture with the organic compound. The 8.84×10^{-4} , a peak current value obtained for the ABA monomer medium, was related to the monomer oxidation of *o*-aminobenzyl alcohol on the SS electrode. The monomer oxidation process in ABA and ORG compound mixture moved to previous potential value, while its current intensities were incredibly high as $1.12 \times 10^{-3} \text{ A}$ than that the presence of only ABA. This case clarifies itself for being a better conductive medium in the presence of ORG compound concerning only the presence of ABA. It showed that the addition of ORG

compound to ABA solution provided an increase in the electropolymerization rate.

Furthermore, because it was not observed an additional oxidation peak in cyclic voltammogram (Figure 2b), we concluded that the organic compound is of high purity. Also, we did not observe the dissolution of the SS electrode for both coated electrodes. On the other hand, the peak current increases obtained for monomer oxidation of coated SS electrodes were significantly high in the first anodic cycles, while their values decreased with increasing cycle numbers. These behaviors of SS electrode in LiClO_4 and ACN medium containing ABA with and without ORG compound could be explained by the lower conductive surface of synthesized PABA film, for the SS electrode surface. Moreover, monomer oxidation peak intensities recorded for ABA + ORG compound mixture were comparatively higher when compared with that of only the ABA medium. After the growth of the polymer film, the process covered the SS electrode surface, a green uniform film for both *o*-aminobenzyl alcohol conditions with and without ORG compound.

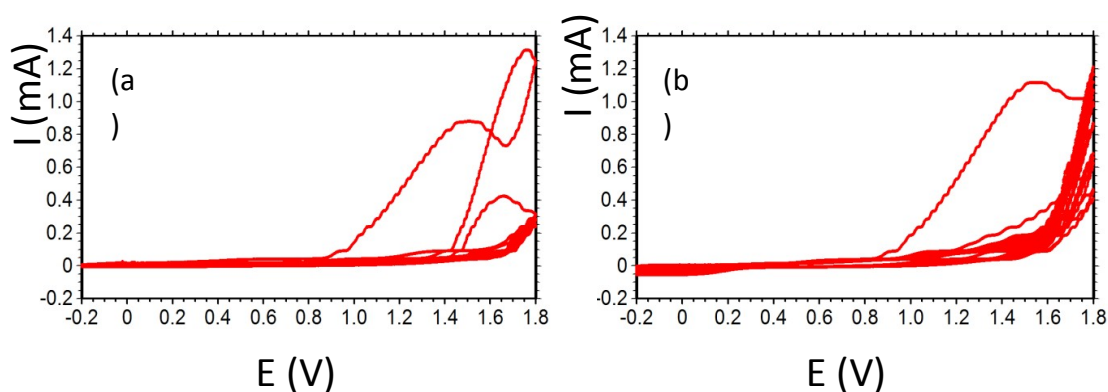


Figure 2: CVs of SS/PABA (a) and SS/PABA-ORG (b) homopolymer film synthesis.

Corrosion protection abilities of coated electrodes

The anticorrosive properties of the PABA and PABA-ORG coated SS electrodes in 3.5 % NaCl were evaluated with EIS, E_{ocp} -time plots, and anodic polarization plot.

We plotted the E_{ocp} values of SS, SS/PABA, and SS/PABA-ORG electrodes against the exposure time at the first half-hour and different exposure times (see Figure 3). Initially, the E_{ocp} measurement of bare SS metal was -0.234 V , while these values recorded for SS/PABA and SS/PABA-ORG electrodes in 3.5 % NaCl electrolyte solution were 0.140 V and 0.070 V , respectively. The E_{ocp} values obtained for uncoated and deposited electrodes shifted to an anodic direction in time. Yet, the E_{ocp} measurements of the SS/PABA-ORG electrode raced to the cathodic direction for a short time after 1654 s of exposure

time. We reported these values of SS/PABA to shift to the positive domain to 0.165 V . Afterwards, according to our observations, the E_{ocp} values of SS/PABA-ORG electrode shifted to the anodic domain from 0.053 to 0.206 V , between 2 and 168 h of exposure time (see Figure 3b). These values recorded for SS/PABA electrode remained constant close to the same potential value for 168 min.

Consequently, we noticed that the SS/PABA-ORG substrate had significantly positive potential region comparison with the only PABA deposited SS metal. We attributed these positive measurements obtained for the SS/PABA-ORG electrode to the formation of, especially nickel and chromium oxide layers, which built up with an extended immersion period, at metal/polymer interface. On the other hand, the E_{ocp} measurements of bare SS metal were carried to the cathodic region from -0.076 to -0.124

V, between 2 and 168 h of immersion period. This case indicated that chloride ions increased the active dissolution of SS the underlying chromium

and nickel oxide layer utilizing its aggressive property and small ion diameter.

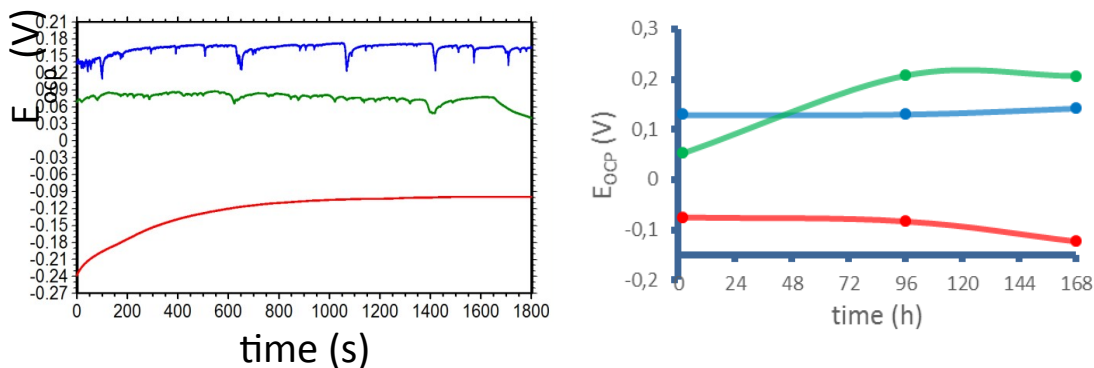


Figure 3: Open circuit potential-time plots of **SS**, **SS/PABA**, and **SS/PABA-ORG** electrodes at first half-hour (a) and different immersion times (b).

Figure 4 compares the anodic polarization plots of SS, SS/PABA, and SS/PABA-ORG substrates after 168 h of exposure period in the solution of corrosion. In the presence of bare SS, we determined the corrosion potential value (E_{corr}) as -0.130 V. Besides, the current values obtained for bare SS were highest when compared with those of coated SS electrodes. This case showed active dissolved of stainless steel in the wider potential region, while current values of the SS electrode remained almost constant in the high potential domain, owing to the formation of chromium and nickel oxide layers. On the other hand, the corrosion potential values of SS/PABA and SS/PABA-ORG electrodes were anodic direction when compared with that of the bare SS electrode. Therefore, this result implied conversion of SS electrode from

anodic dissolution to chromium and nickel oxide layers under the catalyzing effect of polymer film after the corrosive types reached to the SS. The E_{corr} values of polymer film coated electrodes were high due to oxide layers formation and reduction of PABA film. As a result, stabilities of PABA and PABA-ORG coatings were high while permeability was low in aggressive medium and ensured important anodic protection on SS in extended time. Also, the current values of SS/PABA and SS/PABA-ORG electrodes were significantly lower than that of the bare SS electrode. This case showed the effective barrier properties of polymer coatings on the SS electrode. The lowest current values recorded for PABA-ORG coating indicated that ORG compound addition to poly(o-aminobenzyl alcohol) structure exhibited an excellent barrier property on the SS surface.

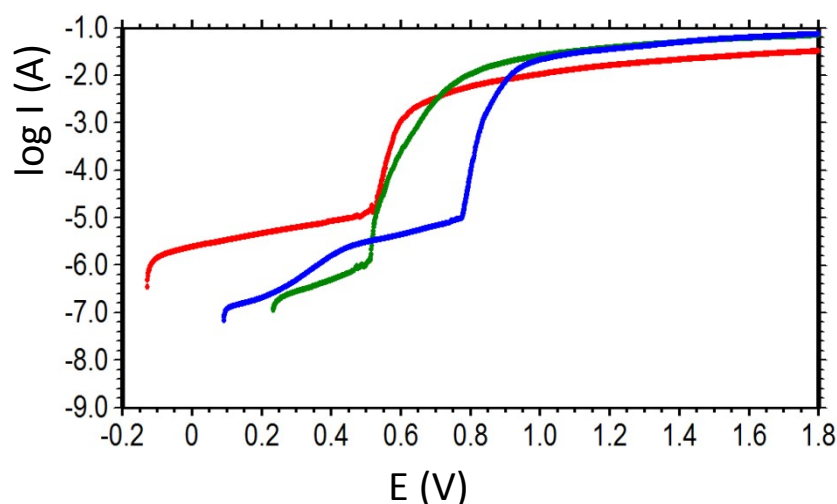


Figure 4: Anodic polarization plots of **SS**, **SS/PABA**, **SS/PABA-ORG** electrodes, after 168h of exposure time.

The Nyquist diagrams obtained for uncoated SS and PABA coated SS (SS/PABA), and PABA-ORG coated

SS are present in Figure 5 for 2, 96, and 168 h of immersion times in the solution of corrosion. There

was a depressed semicircle for metal corrosion at the high-frequency region for bare and deposited electrodes. In Nyquist curves, a one-time constant defined as depressed semicircle at the high-frequency region gave the polarization resistance (R_p). The R_p value obtained for the bare SS electrode was the sum of the resistance of oxide layers (R_o) and the charge transfer resistance (R_{ct}) corresponding to the metal/solution interface formed at the bottom of the pores. In contrast, the fact that almost all curves obtained for coated electrodes were composed of a depressed semicircle gives the R_p value, including the R_o , the R_{ct} , and the polymer film resistance (R_{pf}). Besides, the linear region at the low-frequency side of the Nyquist plots recorded for all of them denoted the presence of Warburg impedance (Z_w) showing a noticeable formation of layers, after 2 h of immersion time in Figure 5a. Warburg impedance assumes the diffusion resistance consisting of corrosion types of the substrate because of being at approx. 45° of angle, in phase angle, $(-)$ -log f plots (14-18). The observation of the linear portion at the low-frequency district showed that the coating had active barrier property.

Consequently, we observed a typical charge transfer process occurring under diffusion control as a linear part. As a result, ion diffusion processes taking place through the pores of the coating and oxide layers towards the underlying metal surface at a metal/solution interface denoted the presence of Warburg impedance. We observed that the bare SS electrode had important anti-corrosion properties due to the formation of stable chromium and nickel oxide layers, after 2 h of the exposure period. In the case of uncoated SS and coated electrodes, there was still a linear portion defined as the Warburg impedance at the lowest frequency domain, which indicated the active protective properties of the oxide and polymer films on surfaces, after 96 h. Nevertheless, we noticed on phase angle-logf plot that the $(-)$ values of coated electrodes obtained a maximal value at approx. 60° (Figure 5b). Higher $(-)$ values of PABA and PABA-ORG polymer film coated SS electrodes attributed to limited corrosive products diffusion process taking place through the

pores of the coating and the formation of new oxide films towards the underlying SS surface at metal/solution interface (14-18). In Figure 5c, the incremental R_p value of depressed semicircle obtained polymer-coated both electrodes at the high frequency indicated the growth of the passive films consisted of nickel and chromium oxides, metal/polymer interface. In the presence of SS/PABA and SS/PABA-ORG electrodes, the one-time constant at high frequency composed of the total resistance of R_{ct} value corresponding to the dissolution of metal at the bottom of the pores, R_{pf} value and R_o value. The linear portion at the low-frequency region of the Nyquist curves denoted the presence of Warburg impedance, pointing out an unusual formation of films (14-18). It is also well known that Warburg coefficient (σ) values give an idea about the diffusability of ion through the polymer film and oxide layers or only the former. We investigated the diffusive properties of polymer films deposited on the SS surface and calculated the Warburg coefficients with details given in the literature (17-18) and (see Table 1). The σ value of SS/PABA and SS/PABA-ORG electrodes was comparatively higher when compared with that of uncoated SS substrate, after 168 h of immersion period (Table 1). We obtained this highest σ value obtained for SS/PABA-ORG electrode by investigation of the $(-)$ -logf plot. In $(-)$ -log f plot, the peak representing polarization resistance expanding between mid and low frequencies in the curve of SS/PABA-ORG electrode indicated the highest phase angle than those of SS/PABA and bare SS electrodes (Figure 5B(c)). So, it was evident that on SS electrode coated with PABA polymer in the organic compound medium had lower porosity structure and number (or only the former), when compared with that of only PABA polymer. As a result, these low porosity properties allowed the limited ion diffusion from the pores of the coating on the metal surface. So, organic compound situated in polymer film structure reduced more the porosity structure of SS electrode by more catalyzing the formation of oxide layers on the SS surface with time. Consequently, the more formation of nickel and chromium oxide layers on the SS surface inhibited mainly the dissolution of stainless steel metal.

Table 1: Corrosion performance values of coated and uncoated SS electrodes, after 168 h period of immersion.

Electrode	E_{OCP} (mV)	R_p (k Ω)	σ ($\Omega \cdot s^{-1/2}$)
SS	-124	5.08	2200.79
SS/PABA	148	30.80	10484.84
SS/PABA-ORG	206	31.16	12576.56

CONCLUSIONS

In this study, we have synthesized PABA film with and without organic compound on the SS surface by cycling the potential in $LiClO_4$ + acetonitrile solution.

The cyclic voltammetric curves demonstrated that PABA coatings synthesized with and without organic compound medium had different morphologic structure and different potential values of monomer oxidation. We investigated the corrosion

performances of SS/PABA and SS/PABA-ORG electrodes in a 3.5 % NaCl solution. It was evaluated with E_{ocp} -time curves, anodic polarization curves, and the AC impedance diagrams and of PABA polymer films synthesized with and without ORG compound obtained on SS surface. This study clearly showed that all the PABA-ORG coating provided valuable protective property against corrosive types such as aggressive chloride ions.

The Nyquist diagrams revealed that PABA-ORG film exhibited significant catalytic efficiency on the formation of protective oxide layers on the SS surface when compared with only PABA film. Consequently, PABA-ORG coating was low permeable and high stability under aggressive chloride medium and ensured exceptional anodic protection on SS over a longer time.

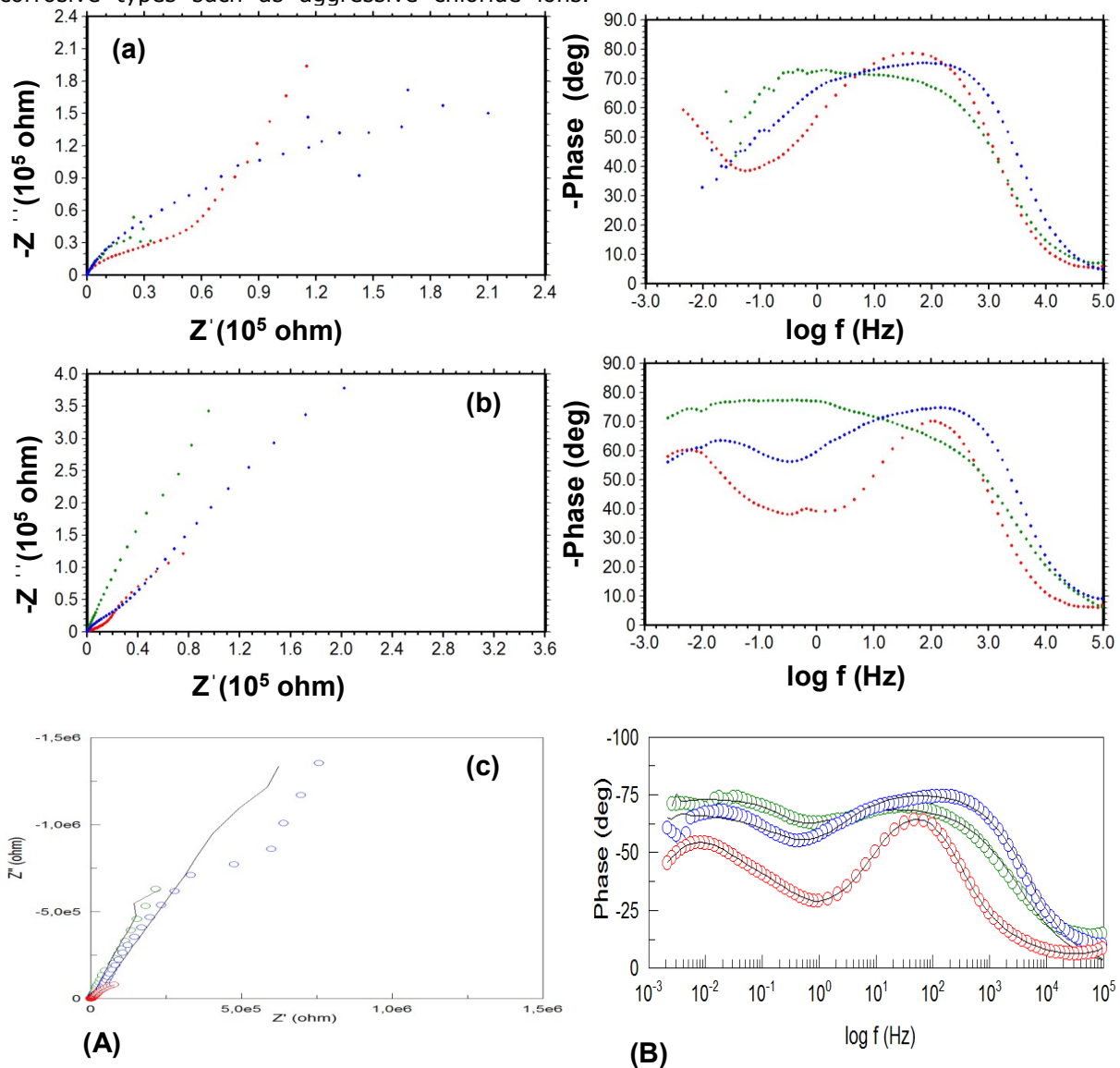


Figure 5: Nyquist (A) and Bode (B) curves recorded for **SS**, **SS/PABA** and **SS/PABA-ORG** electrodes after 2 (a), 96 (b) and 168 (c) h of exposure time in 3.5 % NaCl solution.

ACKNOWLEDGMENTS

This study has been supporting from Hatay Mustafa Kemal University Coordinatorship of Scientific Research Projects by Project No: 19.YL.005. This paper was presented orally at the 2nd International Eurasian Conference on Biological and Chemical Sciences (EurasianBioChem 2019) held in Ankara between 28 – 29 June 2019.

REFERENCES

1. Perez N., *Electrochemistry and Corrosion Science*, Kluwer Academic Publishers, 2004, ISBN: 1-4020-7744-0.
2. Creus J, Mazille H, Idrissi H, Porosity evaluation of protective coatings onto steel, through electrochemical techniques. *Surf. Coat. Technol.*,

- 2000; 130; 224–232. [https://doi.org/10.1016/S0257-8972\(99\)00659-3](https://doi.org/10.1016/S0257-8972(99)00659-3).
3. Sohi MH, Jalali M, Study of the corrosion properties of zinc-nickel alloy electrodeposits before and after chromating. *J. Mater. Process. Tech.* 2003; 138: 63-66, [https://doi:10.1016/S0924-0136\(03\)00050-5](https://doi:10.1016/S0924-0136(03)00050-5).
4. Toprak Doşlu S, Doğru Mert B, Yazıcı B, Polyindole top coat on TiO₂ sol-gel films for corrosion protection of steel. *Corros. Sci.* 2013; 66(8): 51-58, <https://doi.org/10.1016/j.corsci.2012.08.067>.
5. Deshpande PP, Jadhav NG, Gelling VJ, Sazou D, Conducting polymers for corrosion protection: a review. *J. Coat. Technol. Res.* 2014; 11(4): 473–494, <https://doi:10.1007/s11998-014-9586-7>.
6. Ates M, A review on conducting polymer coatings for corrosion protection. *J Adhes. Sci. Technol.*, 2016; 30(14): 1510–1536, <https://doi.org/10.1080/01694243.2016.1150662>.
7. González MB, Saidman SB, Electrodeposition of polypyrrole on 316L stainless steel for corrosion prevention. *Corros. Sci.*, 2011; 53(1): 276–282, <https://doi.org/10.1016/j.corsci.2010.09.021>.
8. Jadhav N, Gelling VJ, Synthesis and Characterization of Micaceous Iron Oxide/Polypyrrole Composite Pigments and Their Application for Corrosion Protection of Cold Rolled Steel. *Corrosion.* 2014;70 (5):464–474, <https://doi.org/10.5006/0980>.
9. Bereket G, Hur E. The Corrosion Protection of Mild Steel by Single Layered Polypyrrole and Multilayered Polypyrrole/Poly(5-amino-1-naphthol) Coatings. *Prog. Org. Coat.* 2009; 65 (1):116–124, <https://doi.org/10.1016/j.porgcoat.2008.10.005>.
10. Bajat JB, Maksimovic MD, Miskovic-Stankovic VB, Zec S, Electrodeposition and characterization of Zn-Ni alloys as sublayers for epoxy coating deposition. *J. Appl. Electrochem.* 2001; 31: 355-361, <https://doi.org/10.1023/A:101758001>.
11. Ozyilmaz AT, Avsar B, Ozyilmaz G, Karahan IH, Camurcu T, Colak F, Different copolymer films on ZnFeCo particles: Synthesis and anticorrosion properties. *Appl. Surf. Sci.* 2014; 318: 262-268, <https://doi.org/10.1016/j.apsusc.2014.04.177>.
12. Ozyilmaz AT, Akdag A, Karahan IH, Ozyilmaz G, The influence of polyaniline (PANI) coating on corrosion behaviour of zinc-cobalt coated carbon steel electrode. *Prog. Org. Coat.* 2013; 76(6): 993-997, <http://doi.org/10.1016/j.porgcoat.2012.10.020>.
13. Bagherzadeh M, Haddadi H, Iranpour M, Electrochemical evaluation and surface study of magnetite/PANI nanocomposite for carbon steel protection in 3.5 % NaCl. *Prog. Org. Coat.* 2016; 101: 149-160, <https://doi.org/10.1016/j.porgcoat.2016.08.011>.
14. Ozyilmaz AT, Aydin AE, Akdag A, Anticorrosive properties with catalytic behaviour of primer PANI film and top PPy coating synthesised in presence of novel norephedrine based amino alcohol compound. *T. I. Met. Finis.* 2014; 92(1): 34-40, <https://doi.org/10.1179/0020296713z.000000000134>.
15. Lorenz WJ, Mansfeld F, Determination of corrosion rates by electrochemical DC and AC methods. *Corros. Sci.* 1981; 21: 647–672, [https://doi.org/10.1016/0010-938x\(81\)90015-9](https://doi.org/10.1016/0010-938x(81)90015-9).
16. Mansfeld F, Use of electrochemical impedance spectroscopy for the study of corrosion protection by polymer-coatings. *Appl. Electrochem.* 1995; 25: 187-202, <http://doi:10.1007/bf00262955>.
17. Walter GW, A review of impedance plot methods used for corrosion performance analysis of painted metals. *Corros. Sci.*, 1986; 26(9): 681-703, [http://doi:10.1016/0010-938x\(86\)90033-8](http://doi:10.1016/0010-938x(86)90033-8).
18. Ozyilmaz AT, Ozyilmaz G, Yigitoglu O, Synthesis and characterization of poly(aniline) and poly(o-anisidine) films in sulphamic acid solution and their anticorrosion properties. *Prog. Org. Coat.* 2010; 67: 28-37. <http://doi:10.1016/j.porgcoat.2009.09.010>.

